A Koopman View on the Harmonic Balance and Hill Method

Fabia Bayer* and Remco I. Leine*
*Institute for Nonlinear Mechanics, University of Stuttgart, Germany

Summary. The Koopman operator provides a way to approximate the dynamics of a nonlinear system by a linear time-invariant system of higher order. In this paper, we aim to study nonlinear time-periodic systems and propose a specific choice of Koopman basis functions combining the Taylor and Fourier bases. This basis allows to recover all equations necessary to perform the Harmonic Balance Method as well as the Hill analysis directly from the linear lifted dynamics. The Mathieu equation and a more general Hill equation are used to exemplify these findings.

Introduction

In the recent years, the Koopman framework and especially its data-driven counterpart, the Extended Dynamic Mode Decomposition, have gained immense popularity [10, 3, 11, 7, 2]. This is due to its auspicious promise: Global representation of a nonlinear system by a linear operator. To this end, in the Koopman framework, the dynamical system is defined through the propagation of functions on the state space, also called observables, over time. While the corresponding operator is linear in its argument, the considered function spaces are usually infinite-dimensional. Therefore, in practice, a linear approximation is considered which is restricted to a finite-dimensional space spanned by a finite number of predefined basis functions. It is well-known that the approximation quality of this restriction strongly depends on the choice of basis functions.
Classically, the Koopman framework is applied to time-autonomous systems $\dot{\mathbf{x}} = \mathbf{f}(\mathbf{x})$ and the approximate linear dynamics obtained by the Koopman lift then takes the form $\dot{\mathbf{z}} = \mathbf{A}\mathbf{z}$. The incorporation of a time-dependent input $\mathbf{v}(t)$ into the dynamics, i.e. $\dot{\mathbf{x}} = \mathbf{f}(\mathbf{x}, \mathbf{v}(t))$ or simply $\dot{\mathbf{x}} = \mathbf{f}(\mathbf{x}, t)$, generally poses problems in the Koopman framework as the system can only be approximated by a linear time-variant system $\dot{\mathbf{z}} = \mathbf{A}\mathbf{z} + \mathbf{B}\mathbf{u}(t)$ if products of state and input are neglected.
In this paper we focus on nonautonomous systems for which the input is time-periodic, i.e. $\mathbf{v}(t) = \mathbf{v}(t+T)$. In particular, we propose a specific choice of observable functions which contains observables depending both on state and time. We demonstrate that this representation contains all frequency information of the system up to some chosen frequency order $N_{\mathbf{u}}$. This means that this basis is a good choice for a Koopman lift, as it retains structural information.
After a short overview about Koopman theory, the specific periodic basis is introduced together with a matching inner product. It is demonstrated how all equations necessary for the Harmonic Balance Method as well as the Hill method follow from the Koopman lift in these specific observables. This means that the (approximate) stability information for the system is retained in the Koopman lift. The findings are illustrated using two variants of the Hill equation.

Koopman theory overview

Consider a nonautonomous time-periodic finite-dimensional dynamical system governed by $\dot{\mathbf{x}} = \mathbf{f}(\mathbf{x}, t)$, where $t \in \mathbb{R}$ is the time, $\mathbf{x}(t) \in \mathcal{X} \subseteq \mathbb{R}^n$ is the state trajectory starting at $\mathbf{x}(t_0) = \mathbf{x}_0$ and $\mathbf{f} : \mathcal{X} \times \mathbb{R} \to \mathcal{X}$ is a smooth vector field which is T-periodic in t. The family of maps $\boldsymbol{\phi}_t(\mathbf{x}_0, t_0) = \mathbf{x}(t)$ characterizes the flow of the system and assigns to each (initial) configuration $(\mathbf{x}_0, t_0)$ the resulting state after time t has passed.
The Koopman framework [10] considers output functions $g(\mathbf{x}, t)$, also called observables. Any spaces of functions over the complex or real numbers are permitted in the general Koopman framework. In this work, we consider in particular the space $\mathcal{F}$ of complex-valued functions $g : \mathcal{X} \times \mathbb{R} \to \mathbb{C}$ which are real analytic on $\mathcal{X}$ and T-periodic in the last argument t.
Given any function g, it may be of interest how its function values evolve along the trajectories of the system. For instance, in the Lyapunov framework, it is desired that function values of a Lyapunov candidate decrease over time for any starting point. The operator $K^t : \mathcal{F} \to \mathcal{F}; g \mapsto g \circ \phi_t$ performs this shift along the trajectory for arbitrary functions g from the considered function space. The family of all these operators for any t is called the Koopman semigroup of operators.
It is easy to see that for suitable $\mathcal{F}$, this Koopman semigroup contains all information about the system without explicitly knowing the vector field $\mathbf{f}$ or the flow $\boldsymbol{\phi}_t$. In particular, if $\mathcal{F}$ is chosen such that the identity function id is contained in the vector space, then the flow can be recovered easily by simply evaluating $K^t(\mathrm{id})$. As a trivial counterexample, consider the one-dimensional vector space of constant functions. Any constant function will not change while being evaluated along an arbitrary trajectory of $\mathbf{x}$. Therefore, in this case, the Koopman operator semigroup is well-defined, albeit trivial. No information about the underlying system is retained. This example shows that an appropriate choice of function space is a crucial part of the Koopman framework.
Under the aforementioned assumptions for the particular function space $\mathcal{F}$ and the vector field $\mathbf{f}$, there also exists the operator $L : \mathcal{F} \to \mathcal{F}, g \mapsto \dot{g}$ mapping an observable g to its total time derivative $\dot{g}$ with

$$\dot{g}(\mathbf{x}, t) = \frac{\partial g(\mathbf{x}, t)}{\partial \mathbf{x}} \mathbf{f}(\mathbf{x}, t) + \frac{\partial g(\mathbf{x}, t)}{\partial t} \ . \tag{1}$$

This operator is called the infinitesimal Koopman generator. Again, for suitable $\mathcal{F}$, this representation alone is a sufficient way to describe the behavior of the dynamical system. In particular, if $\mathrm{id} \in \mathcal{F}$, the vector field $\mathbf{f}$ is easily recovered.
In addition, the Koopman generator and the Koopman semigroup of operators are linear in the argument g, even if the governing differential equation is nonlinear. This comes at the cost of dealing with a mapping on an (infinite-dimensional) function space instead of the (finite-dimensional) state space.
On a finite-dimensional subspace $\mathcal{F}_{\hat{N}} \subset \mathcal{F}$ spanned by $\hat{N}$ linearly independent basis functions $\{\psi_l\}_{l=1}^{\hat{N}}$, any projection $\Pi_{\hat{N}} : \mathcal{F} \to \mathcal{F}_{\hat{N}}$ defines a finite-dimensional approximation $\hat{L} : \mathcal{F}_{\hat{N}} \to \mathcal{F}_{\hat{N}}$ of L on $\mathcal{F}_{\hat{N}}$ by $L_{\hat{N}} := \Pi_{\hat{N}} L$. The approximation process and the subsequent approximation error are visualized in Figure 1. As the subspace $\mathcal{F}_{\hat{N}}$ generally is not closed w.r.t. L, the result of Lg must be projected back to $\mathcal{F}_{\hat{N}}$, introducing some approximation error. Again, the choice of basis functions for $\mathcal{F}_{\hat{N}}$ is crucial. Since $\mathcal{F}_{\hat{N}}$ is finite-dimensional, elements of $\mathcal{F}_{\hat{N}}$ can be represented by a

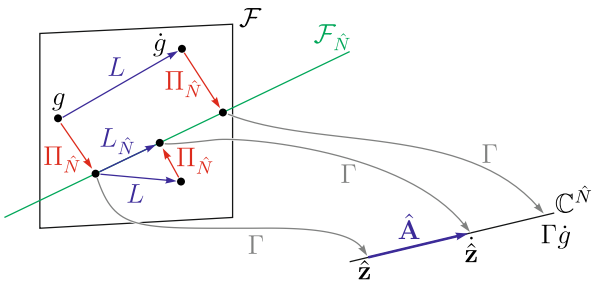

Figure 1: Schematic drawing of the infinitesimal Koopman generator L, its finite-dimensional approximation $L_{\hat{N}}$ and the matrix representation $\hat{\mathbf{A}}$.

column vector of coefficients $\hat{\mathbf{z}} \in \mathbb{C}^{\hat{N}}$. In Figure 1, this is visualized by the map $\Gamma : \mathcal{F}_{\hat{N}} \to \mathbb{C}^{\hat{N}}$. This map can be extended to observables $g \in \mathcal{F} \setminus \mathcal{F}_{\hat{N}}$. In this case, the resulting vector $\hat{\mathbf{z}}$ represents $\Pi_{\hat{N}} g$, which is the projection of g onto $\mathcal{F}_{\hat{N}}$.
The matrix representation of $L_{\hat{N}}$ is $\hat{\mathbf{A}} \in \mathbb{C}^{\hat{N} \times \hat{N}}$ with $\Gamma L_{\hat{N}} g = \hat{\mathbf{A}} \Gamma g$. This matrix also defines a linear time-invariant autonomous differential equation, namely

$$\dot{\hat{\mathbf{z}}} = \hat{\mathbf{A}} \hat{\mathbf{z}} \, . \tag{2}$$

This linear system is called the Koopman lift and describes the dynamics represented in $L_{\hat{N}}$, i.e. it is a finite-dimensional linear approximation of the original system dynamics. The Koopman lift matrix $\hat{\mathbf{A}}$ can be derived from the original nonlinear dynamics manually by using a column vector $\mathbf{\Psi} := \left(\psi_1, \ldots, \psi_{\hat{N}}\right)^{\mathrm{T}}$ of the basis functions of $\mathcal{F}_{\hat{N}}$, computing $\frac{\mathrm{d}\mathbf{\Psi}}{\mathrm{d}t}$ and identifying terms linear in elements of $\mathbf{\Psi}$ after applying the projection $\Pi_{\hat{N}}$. If this projection is orthonormal, the matrix entry $\hat{\mathbf{A}}_{i,j}$ at i-th row and j-th column is given by $\hat{\mathbf{A}}_{i,j} = \left\langle \frac{\mathrm{d}\psi_i}{\mathrm{d}t}, \psi_j \right\rangle$, where $\langle ., . \rangle$ denotes the corresponding inner product.

Koopman lift for time-periodic systems

For smooth autonomous systems in the Koopman framework, it is customary to consider as basis functions a finite set of monomials $\psi_{\boldsymbol{\beta}}(\mathbf{x}) = \mathbf{x}^{\boldsymbol{\beta}}$, where $\boldsymbol{\beta} \in \mathbb{N}^n$ is a multi-index and standard multi-index calculation rules (see, for example, [14, p. 319]) apply. As time-periodic functions are considered in the presented case, we propose in this paper to include as basis functions combinations of polynomial terms as well as Fourier terms of the correct base frequency, i.e. basis functions of the form $\psi_{\boldsymbol{\beta},k} := \mathbf{x}^{\boldsymbol{\beta}} e^{ik\omega t}$, where $\omega = \frac{2\pi}{T}$. The functions $\{\psi_{\boldsymbol{\beta},k} | k \in \mathbb{Z}, \boldsymbol{\beta} \in \mathbb{N}^n\}$ are an orthonormal system within the initially considered vector space $\mathcal{F}$ w.r.t. the inner product

$$\langle g, h \rangle := \int_0^T \left(\frac{1}{(\boldsymbol{\beta}!)^2} \sum_{\boldsymbol{\beta} \in \mathbb{N}^n} \frac{\partial^{\boldsymbol{\beta}} g}{\partial \mathbf{x}^{\boldsymbol{\beta}}}\bigg|_{0,t} \frac{\partial^{\boldsymbol{\beta}} \bar{h}}{\partial \mathbf{x}^{\boldsymbol{\beta}}}\bigg|_{0,t} \right) \mathrm{d}t \, . \tag{3}$$

By slight abuse of notation, the inner product is extended to vector-valued functions $\mathbf{g} \in \mathcal{F}^l$, $\mathbf{h} \in \mathcal{F}^m$ element-wise via

$$\langle \mathbf{g}, \mathbf{h} \rangle := \begin{pmatrix} \langle g_1, h_1 \rangle & \ldots & \langle g_1, h_m \rangle \\ \vdots & \ddots & \vdots \\ \langle g_l, h_1 \rangle & \ldots & \langle g_l, h_m \rangle \end{pmatrix} \, . \tag{4}$$

Let $N_{\boldsymbol{\beta}}, N_{\mathbf{z}}, N_{\mathbf{u}} \in \mathbb{N}$ be integers which describe the assumed maximum polynomial order of the state and maximum frequency order of the state and input, respectively. Let $\{\boldsymbol{\beta}_l\}_{l=1}^{N_{\boldsymbol{\beta}}}$ be a set of multi-indices with $\mathbf{0} \notin \{\boldsymbol{\beta}_l\}_{l=1}^{N_{\boldsymbol{\beta}}}$. For the

sake of brevity, define $N = N_{\boldsymbol{\beta}}(2N_{\mathbf{z}}+1)$. Consider now the specific finite-dimensional subspace $\mathcal{F}_N \subset \mathcal{F}$ spanned by $\boldsymbol{\Psi} = (\boldsymbol{\Psi}_{\mathbf{z}}^{\mathrm{T}}, \mathbf{u}^{\mathrm{T}})^{\mathrm{T}}$ with

$$\boldsymbol{\Psi}_{\mathbf{z}}(\mathbf{x},t) := (\mathbf{x}^{\boldsymbol{\beta}_1} e^{i\omega N_{\mathbf{z}} t}, \dots, \mathbf{x}^{\boldsymbol{\beta}_1} e^{0}, \dots, \mathbf{x}^{\boldsymbol{\beta}_1} e^{-i\omega N_{\mathbf{z}} t}, \mathbf{x}^{\boldsymbol{\beta}_2} e^{i\omega N_{\mathbf{z}} t}, \dots, \mathbf{x}^{\boldsymbol{\beta}_{N_{\boldsymbol{\beta}}}} e^{-i\omega N_{\mathbf{z}} t})^{\mathrm{T}} \tag{5}$$

$$\mathbf{u}(t) := (e^{-i\omega N_{\mathbf{u}} t}, \dots, e^{0}, \dots, e^{i\omega N_{\mathbf{u}} t})^{\mathrm{T}} . \tag{6}$$

It is reasonable to include the state $\mathbf{x}$ itself in the basis such that there is a selector matrix $\mathbf{C}_{\mathbf{z}} \in \mathbb{R}^{n\times N}$ containing some rows of the identity matrix with $\mathbf{C}_{\mathbf{z}}\boldsymbol{\Psi}_{\mathbf{z}}(\mathbf{x},t) = \mathbf{x}$. There exist other options to recover $\mathbf{x}$ if $\mathbf{C}_{\mathbf{z}}$ is allowed to be time-dependent. However, for the considerations of this paper, choosing $\mathbf{C}_{\mathbf{z}}$ to be constant is sufficient. Using the projection defined by the inner product (3), the Koopman lift approximation of the nonlinear system with respect to the basis $\boldsymbol{\Psi}$ is governed by

$$\dot{\hat{\mathbf{z}}} := \begin{pmatrix} \dot{\mathbf{z}} \\ \dot{\mathbf{u}} \end{pmatrix} = \langle \dot{\boldsymbol{\Psi}}, \boldsymbol{\Psi} \rangle \hat{\mathbf{z}} = \begin{pmatrix} \langle \dot{\boldsymbol{\Psi}}_{\mathbf{z}}, \boldsymbol{\Psi}_{\mathbf{z}} \rangle & \langle \dot{\boldsymbol{\Psi}}_{\mathbf{z}}, \mathbf{u} \rangle \\ \langle \dot{\mathbf{u}}, \boldsymbol{\Psi}_{\mathbf{z}} \rangle & \langle \dot{\mathbf{u}}, \mathbf{u} \rangle \end{pmatrix} \begin{pmatrix} \mathbf{z} \\ \mathbf{u} \end{pmatrix} =: \begin{pmatrix} \mathbf{A} & \mathbf{B} \\ * & * \end{pmatrix} \begin{pmatrix} \mathbf{z} \\ \mathbf{u} \end{pmatrix} , \tag{7}$$

where $\mathbf{A} \in \mathbb{C}^{N\times N}$ and $\mathbf{B} \in \mathbb{C}^{N\times(2N_{\mathbf{u}}+1)}$ are constant matrices. The dynamics of $\mathbf{u}$ is approximated by the lower rows of the large matrix in (7). Since $\mathbf{u}$ is state-independent and its time history in (6) is known a priori, the lower rows of (7) are superfluous and the original nonlinear system is approximated by the LTI system $\dot{\mathbf{z}} = \mathbf{A}\mathbf{z} + \mathbf{B}\mathbf{u}$.

Koopman-based Harmonic Balance Method

In the standard Harmonic Balance Method (HBM), a periodic solution is approximated by its Fourier expansion up to order $N_{\mathbf{u}}$ with unknown parameters via

$$\mathbf{x}_p(t) = \sum_{k=-N_{\mathbf{u}}}^{N_{\mathbf{u}}} \mathbf{p}_k e^{ik\omega t} =: \mathbf{P}_{\mathrm{hb}}\mathbf{u} \tag{8}$$

with $\mathbf{u}$ as in (6) and $\mathbf{P}_{\mathrm{hb}} = (\mathbf{p}_{-N_{\mathbf{u}}}, \dots, \mathbf{p}_{N_{\mathbf{u}}})$. The coefficients $\mathbf{p}_k$ are then determined by equating the Fourier expansions of $\frac{\mathrm{d}\mathbf{x}_p}{\mathrm{d}t}$ from the definition (8) and $\mathbf{f}(\mathbf{x}_p,t)$ for every order up to $N_{\mathbf{u}}$. With $(2N_{\mathbf{u}}+1)$ frequencies considered in total, this results in a system of $n(2N_{\mathbf{u}}+1)$ equations for the coefficients in $\mathbf{P}_{\mathrm{hb}}$. While the left-hand side of the equation as well as linear components of $\mathbf{f}$ are easy to handle, the nonlinear components can usually not be expressed analytically. The individual equations for each order are thus usually determined and simultaneously solved using the fast Fourier transform with an alternating frequency and time (AFT) scheme for nonlinear components of $\mathbf{f}$ [4]. However, the equations for each order can also be isolated by projecting onto the corresponding basis function from the collection in $\mathbf{u}$ through the inner product (3). Hence, the HBM approximates a periodic solution by solving the $2N_{\mathbf{u}}+1$ equations collected in

$$\langle \frac{\mathrm{d}\mathbf{x}_p}{\mathrm{d}t}, \mathbf{u} \rangle = \langle \mathbf{f}(\mathbf{x}_p(\cdot),\cdot), \mathbf{u} \rangle . \tag{9}$$

With this notation, it is remarked that the numerically cumbersome task of calculating the Fourier coefficients of the nonlinear components of $\mathbf{f}$ is hidden in the definition of the inner product.

For Koopman-based HBM, again, a periodic orbit with unknown coefficients as in (8) is assumed. Now, the dynamics of a perturbation around this periodic orbit is regarded, i.e. the shifted system with state $\mathbf{y} = \mathbf{x} - \mathbf{x}_p$ is considered. Analogously to the original system, the shifted system can be lifted using the methodology as introduced above. This Koopman lift is of the form (7), with the $\mathbf{A}$ and $\mathbf{B}$ matrices depending on the parameters $\mathbf{p}_k$. Now evaluating only those rows of $\mathbf{z}$ which directly approximate the state $\mathbf{y} \approx \mathbf{C}_{\mathbf{z}}\mathbf{z}$ and using the linearity of the infinitesimal Koopman generator yields

$$\dot{\mathbf{y}}(t) \approx \mathbf{C}_{\mathbf{z}}\dot{\mathbf{z}}(t) = \mathbf{C}_{\mathbf{z}}\mathbf{A}\mathbf{z}(t) + \mathbf{C}_{\mathbf{z}}\mathbf{B}\mathbf{u}(t) = \mathbf{C}_{\mathbf{z}}\mathbf{A}\mathbf{z}(t) + \langle \mathbf{f} - \frac{\mathrm{d}\mathbf{x}_p}{\mathrm{d}t}, \mathbf{u} \rangle \mathbf{u}(t) . \tag{10}$$

As $\mathbf{z} = 0$ implies $\mathbf{y} = 0$ and thus $\mathbf{x} = \mathbf{x}_p$, we have to require that $\dot{\mathbf{y}} = 0$ in this case. As the rows of $\mathbf{u}$ are linearly independent, it follows from (10) that all entries of the inner product, or equivalently of the matrix $\mathbf{B}$, must then be zero. Thus, by comparing (9) and (10), the HBM equations are exactly given by $\mathbf{C}_{\mathbf{z}}\mathbf{B} = \mathbf{0}$ for the Koopman lift as introduced.

Stability Analysis

When a periodic orbit $\mathbf{x}_p$ is found (via HBM or otherwise), the next interesting question is that of its stability properties; that is, whether trajectories that start sufficiently close to the periodic orbit will approach it, stay close to it or tend away from it with increasing time. To evaluate the stability properties, the dynamics of a perturbation $\mathbf{y} = \mathbf{x} - \mathbf{x}_p$ from the periodic solution is considered. Substitution of this definition into the original system yields

$$\dot{\mathbf{y}} = \mathbf{f}(\mathbf{x}_p + \mathbf{y}) - \dot{\mathbf{x}}_p := \mathbf{J}(t)\mathbf{y} + \mathcal{O}(\|\mathbf{y}\|^2) , \tag{11}$$

where $\mathbf{J}(t) = \frac{\partial \mathbf{f}}{\partial \mathbf{x}}\big|_{t,\mathbf{x}_p(t)}$ is the system Jacobian. This system has an equilibrium at zero, which corresponds to the periodic orbit of the original system, and the stability analysis of the periodic orbit reduces to the stability analysis of this equilibrium. To make qualitative (stability/instability) statements around the origin, it is usually sufficient to discard higher-order terms and only regard the linearized time-varying perturbation equation $\dot{\mathbf{y}} = \mathbf{J}(t)\mathbf{y}$. This will be the convention for the remainder of this paper unless stated otherwise.
The fundamental solution matrix $\mathbf{\Phi}(t)$ is the solution to the variational equation

$$\dot{\mathbf{\Phi}}(t) = \mathbf{J}(t)\mathbf{\Phi}(t)\,; \qquad \mathbf{\Phi}(0) = \mathbf{I} \tag{12}$$

and any state can be obtained via $\mathbf{y}(t) = \mathbf{\Phi}(t)\mathbf{y}_0$. In particular, the fundamental solution matrix $\mathbf{\Phi}(T) := \mathbf{\Phi}_T$ is called the monodromy matrix of the system and its eigenvalues $\{\lambda_k\}_{k=1}^n$ are called Floquet multipliers [15]. The Poincaré map $\mathbf{y}_{k+1} = \mathbf{\Phi}_T\mathbf{y}_k$ provides snapshots for the evolution of the perturbation $\mathbf{y}$, spaced at a time distance of T. Therefore, stability analysis of the linear time-periodic system reduces to stability analysis of the Poincaré map. Hence, if all Floquet multipliers are of magnitude strictly less than one, the equilibrium of the LTV system and thus the periodic solution of the original system are stable; if at least one eigenvalue has a magnitude strictly larger than one, they are unstable.
Alternatively to the Floquet multipliers, the stability properties of a time-periodic linear system can be characterized by the Floquet exponents. In the linear system as above there exist n solutions $\mathbf{y}_k(t) = \mathbf{p}_k(t)e^{\alpha_k t}$, where $\mathbf{p}_k$ is T-periodic [15]. Hence, stability is characterized by the real parts of the Floquet exponents $\{\alpha_k\}_{k=1}^n$. If at least one Floquet exponent lies in the open right half plane, i.e. if at least one real part is larger than zero, the equilibrium is unstable. These Floquet exponents are not uniquely defined. It is easy to see that if $\mathbf{p}_k(t), \alpha_k$ generate a solution $\mathbf{y}_k(t)$, the same solution is generated by $\tilde{\alpha}_k = \alpha_k + il\omega$ and $\tilde{\mathbf{p}}_k(t) = \mathbf{p}_k(t)e^{-il\omega t}$ with $l \in \mathbb{Z}$. Hence, in total, there are infinitely many valid Floquet exponents, which can be categorized into n distinct groups. As all entries of one group have the same real part, it is sufficient for stability analysis to know any one entry from each of the n groups.

Hill method

When a periodic orbit is determined using the purely time-domain-based shooting method, the monodromy matrix is a direct byproduct of the continuation method [13]. In this case, the numerically obtained monodromy matrix can be evaluated directly to obtain the Floquet multipliers and their stability information.
When the Harmonic Balance Method is computed in the standard way, however, stability information about the identified limit cycle is unclear without further investigation. The Hill method offers a frequency-domain-based way to approximate the Floquet exponents of the linearized perturbation equation.
The Floquet exponents are eigenvalues of the infinite Hill matrix $\mathbf{H}_\infty$ [8], which is constructed from the Fourier coefficients of $\mathbf{J}(t) = \sum_{k=-\infty}^{\infty} \mathbf{J}_k e^{i\omega k t}$ and reads as

$$\mathbf{H}_\infty = \begin{pmatrix} \ddots & \vdots & \vdots & \vdots & \iddots \\ \dots & \mathbf{J}_0 + i\omega\mathbf{I} & \mathbf{J}_{-1} & \mathbf{J}_{-2} & \dots \\ \dots & \mathbf{J}_1 & \mathbf{J}_0 & \mathbf{J}_{-1} & \dots \\ \dots & \mathbf{J}_2 & \mathbf{J}_1 & \mathbf{J}_0 - i\omega\mathbf{I} & \dots \\ \iddots & \vdots & \vdots & \vdots & \ddots \end{pmatrix}. \tag{13}$$

This infinite-dimensional eigenproblem has infinitely many discrete eigenvalues. They correspond identically to the Floquet exponents $\tilde{\alpha}$ for all $l \in \mathbb{Z}$ as introduced above and can be sorted into n groups, where the entries of each group differ by multiples of $i\omega$ [12]. However, in practice, only the eigenvalues of a finite-dimensional matrix approximation of $\mathbf{H}_\infty$ can be computed numerically. The matrix

$$\mathbf{H} = \begin{pmatrix} \mathbf{J}_0 + iN\omega\mathbf{I} & \mathbf{J}_{-1} & \dots & \mathbf{J}_{-2N} \\ \mathbf{J}_1 & \mathbf{J}_0 + i(N-1)\omega\mathbf{I} & \dots & \mathbf{J}_{-2N+1} \\ \vdots & \vdots & \ddots & \vdots \\ \mathbf{J}_{2N} & \mathbf{J}_{2N-1} & \dots & \mathbf{J}_0 - iN\omega\mathbf{I} \end{pmatrix} \tag{14}$$

of size $N \times N$ (recall $N = n(2N_\mathbf{u} + 1)$) consists of the N most centered rows and columns of $\mathbf{H}_\infty$ and approximates the original infinite-dimensional matrix. In the absence of truncation error, the eigenvalues of $\mathbf{H}$ are some subset of the eigenvalues of $\mathbf{H}_\infty$, i.e. the Floquet exponents. Due to the inevitable error which generally comes with truncation, however, this does not quite hold. The N eigenvalues of $\mathbf{H}$ will be called Floquet exponent candidates below.
The matrix $\mathbf{H}$ has a block Toeplitz structure and for sufficiently large $N_\mathbf{u}$, the bands near the diagonal dominate as the Fourier coefficients of $\mathbf{J}$ tend to zero for $N_\mathbf{u}$ large enough. Loosely speaking, this means that some eigenvalues affiliated most with the central rows of $\mathbf{H}$ are less impacted by the truncation and provide a better approximation to the Floquet exponents than others. The search for a selection criterion which determines the best approximation to the Floquet exponents from the Floquet candidates has received much attention in the literature [5, 16, 8, 12].
For sufficiently large $N_\mathbf{u}$, it is proven that the candidates with lowest imaginary part in modulus converge to the true Floquet exponents [16]. An alternative criterion selects those candidates whose eigenvectors are most symmetric [8, 6], as

they should correspond most to the middle rows of the block Toeplitz matrix $\mathbf{H}$. Even though there currently is no formal convergence proof for this symmetry-based sorting method, numerical results indicate faster convergence than with the aforementioned eigenvalue criterion [1].
For both these criteria, all eigenpairs of the large matrix have to be computed first and then most of them are discarded. As the cost of solving an eigenvalue problem is of the order $\mathcal{O}(N^3)$, the computational cost of the approach is usually dominated by determining the eigendecomposition of a large matrix.

Koopman-based Hill method
Consider again the lifted perturbation dynamics (10) around a periodic solution. As explained above, for a periodic solution, the matrix $\mathbf{B}$ should vanish and the autonomous system $\dot{\mathbf{z}} = \mathbf{A}\mathbf{z}$ remains. After the coefficients $\mathbf{p}_k$ of the periodic solution are substituted into $\mathbf{A}$, it is a matrix with purely numerical entries. Let $\mathbf{C}_\mathrm{H}$ denote the real selection matrix sorting all terms in $\mathbf{\Psi_z}$ which are linear in $\mathbf{x}$ such that

$$\mathbf{C}_\mathrm{H}\mathbf{\Psi_z}(\mathbf{y},t) = \left(\mathbf{y}^\mathrm{T}e^{iN\omega t}, \mathbf{y}^\mathrm{T}e^{i(N-1)\omega t}, \dots, \mathbf{y}^\mathrm{T}e^{-iN\omega t}\right)^\mathrm{T} . \tag{15}$$

Entries in $\mathbf{C}_\mathrm{H}\mathbf{\Psi_z}$ are of the form $\mathbf{y}e^{-ik\omega t}$ and are sorted by ascending k ranging from $-N$ to N. Note that $\frac{\partial(\mathbf{C_H}\mathbf{\Psi_z})}{\partial t} = \mathbf{\Omega}\mathbf{C_H}\mathbf{\Psi_z}$ with $\mathbf{\Omega} = \mathrm{diag}\left(iN\omega, i(N-1)\omega, \dots, -iN\omega\right)$. The matrix $\mathbf{C}_\mathrm{H}\mathbf{A}\mathbf{C}_\mathrm{H}^\mathrm{T}$ can be rearranged using the definition (7). After block-wise differentiation of $\mathbf{C}_\mathrm{H}\mathbf{\Psi_z}$, the Jacobian $\mathbf{J}$ is expressed by its Fourier expansion. Finally, after identifying terms corresponding to $(\mathbf{C}_\mathrm{H}\mathbf{\Psi_z})$ in the first argument of the inner product, it follows that

$$\mathbf{C}_\mathrm{H}\mathbf{A}\mathbf{C}_\mathrm{H}^\mathrm{T} = \left\langle \frac{\mathrm{d}\left(\mathbf{C}_\mathrm{H}\mathbf{\Psi_z}\right)}{\mathrm{d}t}\mathbf{C}_\mathrm{H}^\mathrm{T}, \mathbf{\Psi_z} \right\rangle = \left\langle \left(\frac{\partial \mathbf{C}_\mathrm{H}\mathbf{\Psi_z}}{\partial \mathbf{y}}\mathbf{J}\mathbf{y} + \frac{\partial \mathbf{C}_\mathrm{H}\mathbf{\Psi_z}}{\partial t} \right), \mathbf{C}_\mathrm{H}\mathbf{\Psi_z} \right\rangle = \mathbf{H} . \tag{16}$$

Thus, all stability information obtained for a time-periodic system by the Hill method is also contained in the Koopman lift of the system. In particular, if $\mathbf{\Psi_z}$ only contains terms that are linear in $\mathbf{x}$ and not of higher polynomial orders, then $\mathbf{C_H}$ is quadratic and orthogonal. This makes (16) a similarity transform and it can be concluded that the eigenvalues of $\mathbf{A}$ are identical to those of $\mathbf{H}$, i.e. the Floquet candidates.

Examples

Two variants of the Hill equation $\ddot{x} + g(t)x = 0$ with $g(x)$ being 2π-periodic are used to exemplify and illustrate the properties discussed above. First, the Koopman lift for the scalar Mathieu equation with $g(t) = a + 2b\cos(2\omega t)$ is provided explicitly for the lowest possible $N_\mathbf{u}$ as an example for the structure both in the $\mathbf{A}$ and the $\mathbf{B}$ matrix. The stability properties of the Mathieu equation are then investigated using both a HBM variant and the Floquet exponents retrieved from the Koopman lift. Finally, a more complicated expression for g is analyzed to illustrate the impact of the choice of $N_\mathbf{u}$.

Mathieu equation
As an example, consider the scalar Mathieu equation $\ddot{x} + (a + 2b\cos(2t))x = 0$. In the (a,b)-space, regions of stability and instability are separated by branches of nontrivial periodic solutions [9], which are visualized in a so-called Ince-Strutt diagram.
For treatment in the Koopman framework, the system is brought to first-order form with $\mathbf{x} = (x, \dot{x})^\mathrm{T}$. The first-order dynamics is then of the form

$$\dot{\mathbf{x}} = \mathbf{J}(t)\mathbf{x} = \begin{pmatrix} 0 & 1 \\ -a - 2b\cos(2t) & 0 \end{pmatrix}\mathbf{x} = \left[\begin{pmatrix} 0 & 1 \\ -a & 0 \end{pmatrix} + \begin{pmatrix} 0 & 0 \\ -b & 0 \end{pmatrix}\left(e^{i\omega t} + e^{-i\omega t}\right) \right]\mathbf{x} . \tag{17}$$

The Fourier decomposition of $\mathbf{J}(t)$ can be read directly from (17). Assume a periodic solution $\mathbf{x}_p = \mathbf{x} - \mathbf{P}_\mathrm{hb}\mathbf{u}$ with $\mathbf{u}$ as in (6) and $\mathbf{P}_\mathrm{hb}$ collecting the $\mathbf{p}_k$ from HBM column-wise. Choose a vector of basis observables $\mathbf{\Psi_z}$ which only contains terms linear in $\mathbf{x}$. For readability of the result, assume that $\mathbf{\Psi_z}$ is already sorted as in (15). Hence, in this case, $\mathbf{C}_\mathrm{H}$ is the identity matrix. The selection matrix $\mathbf{C_z}$ is of the form

$$\mathbf{C_z} = \begin{pmatrix} 0 & \dots & 0 & 1 & 0 & 0 & \dots & 0 \\ 0 & \dots & 0 & 0 & 1 & 0 & \dots & 0 \end{pmatrix} \tag{18}$$

with a 2×2 identity matrix in the middle, surrounded by blocks of zeros with $2N_\mathbf{u}$ columns each. Performing the Koopman lift (7) on $\mathbf{y} = \mathbf{x} - \mathbf{x}_p$ yields for $N_\mathbf{u} = 1$ the linear time-invariant system

$$\dot{\mathbf{y}} \approx \mathbf{C_z}(\mathbf{A}\mathbf{z} + \mathbf{B}\mathbf{u}) = \mathbf{C_z}\begin{pmatrix} i\omega & 1 & 0 & 0 & 0 & 0 \\ -a & i\omega & 0 & 0 & -b & 0 \\ 0 & 0 & 0 & 1 & 0 & 0 \\ 0 & 0 & -a & 0 & 0 & 0 \\ 0 & 0 & 0 & 0 & -i\omega & 1 \\ -b & 0 & 0 & 0 & -a & -i\omega \end{pmatrix}\mathbf{z} + \left[\mathbf{A}_{3:4}\begin{pmatrix} \mathbf{p}_{-1} \\ \mathbf{p}_0 \\ \mathbf{p}_1 \end{pmatrix} \; \mathbf{A}_{5:6}\begin{pmatrix} \mathbf{p}_{-1} \\ \mathbf{p}_0 \\ \mathbf{p}_1 \end{pmatrix} \; \mathbf{A}_{1:2}\begin{pmatrix} \mathbf{p}_{-1} \\ \mathbf{p}_0 \\ \mathbf{p}_1 \end{pmatrix} \right]\mathbf{u}, \tag{19}$$

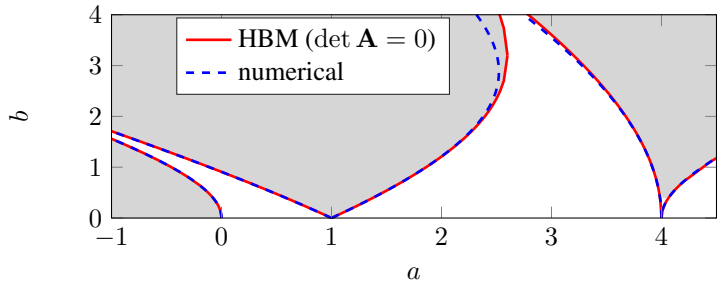

Figure 2: Ince-Strutt diagram for the Mathieu equation. Stable (unstable) regions determined by Koopman-based Hill method of order 4 in white (gray). Transition curves, i.e. parameter combinations which admit nontrivial periodic solutions, determined by Koopman-based HBM (solid red) and numerically using a shooting procedure (dashed blue).

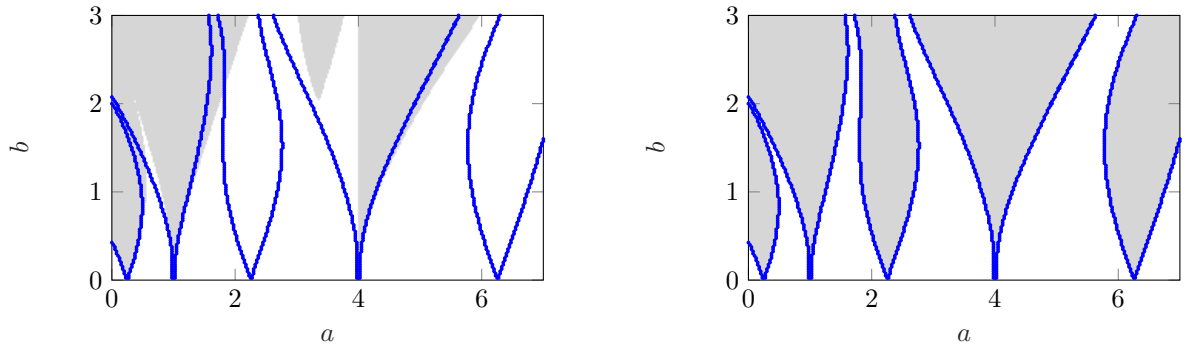

(a) $N_{\mathbf{u}} = 2$ (b) $N_{\mathbf{u}} = 10$

Figure 3: Stability charts for the more complicated Hill's equation (20). Stable (unstable) regions determined by Koopman-based Hill method in white (gray). Transition curves determined by direct numerical integration of the variational equation (12) in blue.

where $\mathbf{A}_{i:j}$ denotes the i-th to j-th rows of $\mathbf{A}$. Hence, all rows of $\mathbf{A}$ reoccur in $\mathbf{C_z B}$. The entries in $\mathbf{A}$ do not depend on $\mathbf{p}_k$ in this special case. This is because the original dynamics of the Mathieu equation is linear in the state. As the linear time-varying system has an equilibrium at $\mathbf{x} = \mathbf{0}$, the HBM equations coded in $\mathbf{C_z B}$ are a homogeneous linear equation system for the parameters $\mathbf{p}_k$. The system only has nontrivial periodic solutions on the stability boundary curves. If the dynamical system has a nontrivial periodic solution, then the linear equation system resulting from HBM must have one as well. This means that the determinant of this linear equation system, or equivalently that of $\mathbf{A}$, must vanish. This is an approximate algebraic condition for the transition curves which separate stable and unstable regions in the Ince-Strutt diagram based on the HBM using the Koopman lift of the system.
In the $\mathbf{A}$ matrix, the 2×2 block Toeplitz structure of (14) is clearly visible. With the Hill method, this can also be used to approximate the stability regions using the Floquet candidates found as eigenvalues of $\mathbf{A}$. Here, the eigenvalues of $\mathbf{A}$ with lowest imaginary part in modulus were used as Floquet exponent approximations. For the case $N_{\mathbf{u}} = 4$, the stability regions and transition curves found by the Koopman-based HBM and Koopman-based Hill method are pictured in Figure 2. In the white regions, the two eigenvalues of $\mathbf{A}$ with imaginary part closest to zero both have a real part of zero, while in the gray regions, one has a real part larger than zero and the other has a real part smaller than zero. A comparison with numerically obtained transition curves using a shooting procedure based on [9] shows good approximation quality for the first instability tongues already for small $N_{\mathbf{u}}$.
Below, we consider the more complicated Hill's equation

$$g(t) = a + b(\sin(t) + \sin(8t) + \cos(5t) + \cos(3t)) \ . \tag{20}$$

In contrast to the previous Mathieu equation, higher frequencies are part of the dynamics. This means that the matrix $\mathbf{A}$ of the Koopman lift (or, equivalently, the $\mathbf{H}$ matrix of the Hill method) exhibits a diagonal band structure only if $N_{\mathbf{u}}$ is chosen larger than before. Additionally, block symmetry in $\mathbf{A}$ is lost. As expected it is visible in Figures 3a and 3b that low orders of $N_{\mathbf{u}}$ are now not sufficient to capture the dynamics. Higher orders of $N_{\mathbf{u}}$, however, do capture the stability regions accurately.

Conclusion

In the Koopman framework, the choice of observables plays a crucial role for the accuracy of the final finite-dimensional Koopman lift. In this work, the connection between a specific choice of Koopman observables based on Taylor as well

as Fourier monomials and established frequency domain tools for the analysis of time-periodic nonlinear systems is highlighted. This connection motivates the use of this type of observables in a Koopman-based setting and provides some legitimization. In further research, this connection could be utilized to carry over structural insights from the original nonlinear system into its frequency representation.

References

[1] B. Bentvelsen and A. Lazarus. Modal and stability analysis of structures in periodic elastic states: application to the Ziegler column. *Nonlinear Dynamics*, 91(2):1349–1370, 2018.

[2] D. Bruder, X. Fu, R. B. Gillespie, C. D. Remy, and R. Vasudevan. Data-driven control of soft robots using Koopman operator theory. *IEEE Transactions on Robotics*, 37(3):948–961, 2021.

[3] M. Budišić, R. Mohr, and I. Mezić. Applied Koopmanism. *Chaos: An Interdisciplinary Journal of Nonlinear Science*, 22(4):047510, 2012.

[4] T. M. Cameron and J. H. Griffin. An alternating frequency/time domain method for calculating the steady-state response of nonlinear dynamic systems. *J. Appl. Mech*, 56(1):149–154, 1989.

[5] T. Detroux, L. Renson, L. Masset, and G. Kerschen. The harmonic balance method for bifurcation analysis of large-scale nonlinear mechanical systems. *Computer Methods in Applied Mechanics and Engineering*, 296:18–38, 2015.

[6] L. Guillot, A. Lazarus, O. Thomas, C. Vergez, and B. Cochelin. A purely frequency based Floquet-Hill formulation for the efficient stability computation of periodic solutions of ordinary differential systems. *Journal of Computational Physics*, 416:109477, 2020.

[7] M. Korda and I. Mezić. On convergence of extended dynamic mode decomposition to the Koopman operator. *Journal of Nonlinear Science*, 28(2):687–710, 2018.

[8] A. Lazarus and O. Thomas. A harmonic-based method for computing the stability of periodic solutions of dynamical systems. *Comptes Rendus Mécanique*, 338(9):510–517, 2010.

[9] R. I. Leine. Non-smooth stability analysis of the parametrically excited impact oscillator. *International Journal of Non-Linear Mechanics*, 47(9):1020–1032, 2012.

[10] A. Mauroy, Y. Susuki, and I. Mezić. Introduction to the Koopman operator in dynamical systems and control theory. In *The Koopman Operator in Systems and Control. Concepts, Methodologies and Applications*, pages 3–33. Cham: Springer, 2020.

[11] I. Mezic. On applications of the spectral theory of the Koopman operator in dynamical systems and control theory. In *54th IEEE Conference on Decision and Control, CDC 2015, Osaka, Japan, December 15-18, 2015*, pages 7034–7041. IEEE, 2015.

[12] G. Moore. Floquet theory as a computational tool. *SIAM Journal on Numerical Analysis*, 42(6):2522–2568, 2005.

[13] M. Peeters, R. Viguié, G. Sérandour, G. Kerschen, and J.-C. Golinval. Nonlinear normal modes, Part II: Toward a practical computation using numerical continuation techniques. *Mechanical Systems and Signal Processing*, 23(1):195–216, 2009.

[14] M. Reed and B. Simon. *Functional Analysis*. Number 1 in Methods of Modern Mathematical Physics. Academic Press, revised and enlarged edition, 1980.

[15] G. Teschl. *Ordinary Differential Equations and Dynamical Systems*. Number 140 in Graduate Studies in Mathematics. American Mathematical Society, Providence, Rhode Island, 2012.

[16] J. Zhou, T. Hagiwara, and M. Araki. Spectral characteristics and eigenvalues computation of the harmonic state operators in continuous-time periodic systems. *Systems & Control Letters*, 53(2):141–155, 2004.